4-2018

The Impact of the 515nm Effect on 1O2 Quenching in Photosynthesis: Model System Studies Using β-Carotene–Acid Complexes

Lauren A. Hoody
University of Dayton

The Impact of the 515nm Effect on $^1O_2$ Quenching in Photosynthesis: Model System Studies Using β-Carotene–Acid Complexes

Honors Thesis

Lauren A. Hoody

Department: Chemistry

Advisor: Mark Masthay, Ph.D.

April 2018

The Impact of the 515nm Effect on $^1O_2$ Quenching in Photosynthesis: Model System Studies Using β-Carotene–Acid Complexes

Honors Thesis

Lauren A. Hoody

Department: Chemistry

Advisor: Mark Masthay, Ph.D.

April 2018

Abstract

β-carotene (βC) is an orange pigment present in the photosynthetic reaction center (PRC) of green plants, where it plays a vital role in photosynthesis: It quenches singlet oxygen ($^1O_2$, a toxic oxidizing species generated during photosynthesis) before the $^1O_2$ damages chlorophyll and other components of the PRCs. During photosynthesis, βC temporarily converts from its native *orange–450* state to a *pink–515* state via the so–called *515nm Effect.* Because of the differences between the electronic structures of orange–450 and pink–515, I hypothesize that pink–515 will quench $^1O_2$ less efficiently than orange–450. This hypothesis has not been tested to date because orange–450 and pink–515 states are both inherently present during photosynthesis, making deconvoluation of their relative $^1O_2$–quenching efficiencies affectively impossible. The object of this research was to chemically model βC's pink state with blue βC–acid complexes, which are chemically similar to pink βC, created by reacting βC with trichloroacetic acid (TCA), in order to test this hypothesis. βC's efficiency at deactivating $^1O_2$ was characterized by measuring the rate of degradation of 1,3-diphenylisobenzofuran (DPBF), which has a high reactivity towards $^1O_2$ and is used to detect the amount of $^1O_2$ in a solution. Our DPBF–based results to date indicate that native orange βC and blue βC–TCA complexes quench $^1O_2$ with roughly equal efficiency, with the native orange βC showing slightly more efficiency in ability to quench $^1O_2$. In future studies, we intend to confirm our DPBF–based results by monitoring the impact of βC and βC–TCA complexes on the 1270 nm (near–infrared) emission of $^1O_2$ using a cooled photomultiplier tube. The results from this research will further the understanding of the 515nm Effect and βC's role in photosynthesis and could facilitate the development of solar energy devices with greater long-term stability.

UNIVERSITY of DAYTON

Table of Contents

INTRODUCTION

β–carotene ($C_{40}H_{56}$, see Fig. 1; βC hereafter) is a naturally–occurring biological pigment responsible for the orange color of "orange" and "yellow" fruits and vegetables such as carrots, squash, and oranges.[1] It is also present in the photosynthetic reaction centers (PRCs) of green plants where it plays an essential photoprotective role: βC rapidly "quenches" singlet oxygen ($^1O_2$, a toxic oxidizing species which is generated as a by–product of photosynthesis), thereby preventing oxidative damage to the PRCs.[1] (See Appendix I for details [1-4]).

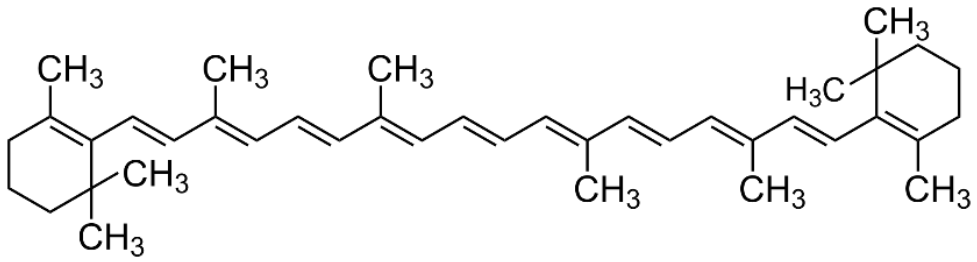

Figure 1. β–carotene (βC; $C_{40}H_{56}$).

In its native *orange–450* state, βC has a wavelength absorption maximum (λ_{max}) of 450 nm. The λ_{max} increases by 65nm as βC converts from the orange–450 state to a transient *pink–515* state (λ_{max} = 515nm) for approximately 0.01 seconds during the photosynthetic cycle.[2-4] This so–called *515nm Effect* is expected to decrease the $^1O_2$–quenching efficiency $\square_Q$ of βC during the brief periods in the photosynthetic cycle when βC is in its pink–515 state; (i.e. $\Phi_Q^{pink\text{–}515} < \Phi_Q^{orange\text{-}450}$).

Since the 515nm Effect is inherent to photosynthesis, both the native orange–450 and pink–515 states of βC contribute to $^1O_2$–quenching in PRCs; in studies of green plants, then, it is not possible to deconvolute $\Phi_Q^{pink-515}$ from $\Phi_Q^{orange-450}$. Even so, by using

model systems which—like the pink–515 state—are red–shifted with respect to the native orange–450 state, the impact of the 515nm Effect on $^1O_2$–quenching can be inferred.

In this research, the pink–515 state will be modeled using *Blue βC–Acid Complexes* (βC–ACs)—in which the native orange–450 state of βC is converted to a *blue–900* state (see Fig. 2 & Fig. 3) by various acids.[5-12] βC–ACs are particularly good models for the pink–515 state, for two reasons: (1) the efficiency of $^1O_2$–quenching is expected to vary inversely with the λ_{max} of the quencher (*i.e.*, $\Phi_Q^{color-\lambda_{max}} \propto \lambda_{max}^{-1}$); and (2) the red shift for the blue–900 state is greater than that for the pink–515 state, therefore mimicing and exaggerating the 515nm Effect. Hence, the blue–900 state is expected to be a poorer $^1O_2$–quencher than the pink–515 state; the quenching efficiencies are thus expected to follow the trend $\Phi_Q^{orange\text{-}450} > \Phi_Q^{pink\text{–}515} > \Phi_Q^{blue\text{–}900}$.

Figure 2. (Left) A 10^{-5}M solution of β-carotene (βC) in its native *orange-450* state in benzene solvent; (right) A solution of the *blue-900* βC-TFA complex in benzene solvent, with [βC] = 10^{-5}M and [TFA] = 0.5M (TFA = trifluoroacetic acid).

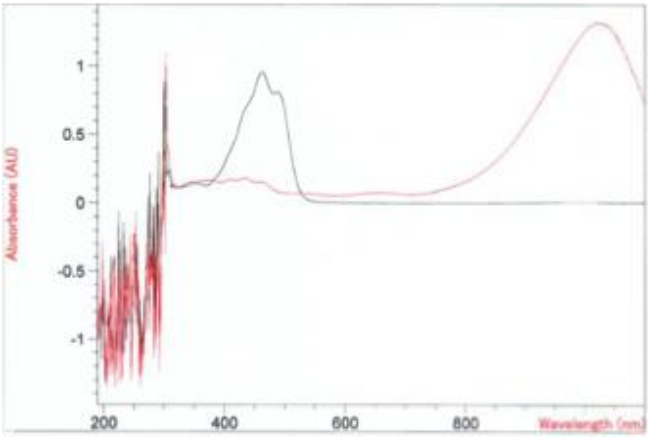

Figure 3. (Black) Absorption spectrum of 10^{-5}M βC in benzene solvent in its native orange-450 state. (Red) The same solution in the presence of 0.5M TFA, illustrating the acid-induced +450 nm bathochromic shift as βC converts to the *blue-900* species. This shift significantly exceeds the +65 nm bathochromic shift observed when photosynthetic systems undergo the *515nm Effect*. The "noisiness" of the spectra at $\lambda <$ 300nm is due to absorption by benzene solvent, which has a UV cutoff of 280 nm, below which %T ≤ 10%.

My research was designed to test a single, central working hypothesis—namely, that the $^1O_2$–quenching efficiency of βC is maximized for its native orange–450 state and decreases with increasing λ_{max}. This hypothesis would be verified if experiments indicate that $\Phi_Q^{blue\text{–}900} < \Phi_Q^{orange\text{-}450}$. Because the pink–515 and acid blue–900 states have similar electronic structure, confirmation of our working hypothesis will strongly suggest that the 515 Effect decreases the efficiency of $^1O_2$–quenching in photosynthesis.

Two techniques may be used in order to test this hypothesis: (1) A state-of-the-art photometric-based technique using a cooled photomultiplier tube to determine the amount of $^1O_2$ present in solutions by measuring the intensities I_{1270} of $^1O_2$ at 1270nm, and (2) An older, chemically-based technique using the $^1O_2$ substrate 1,3-Diphenylisobenzofuran (DPBF) to determine the amount of $^1O_2$ present in solutions by measuring the rate of degradation of DPBF. This project required many steps to optimize the system both chemically and optically. The chemical optimization of our system is complete: the system used utilizes acid blue–900 species comprised of 10^{-5}M βC combined with 0.5M trichloroacetic acid (TCA) with $5*10^{-5}$M C_{60} as the $^1O_2$

photosensitizer, all dissolved in benzene solvent. Unfortunately, because of unexpected difficulties with I_{1270} measurements using the *NIRQuest*, we have not yet been able to characterize the 1270nm phosphorescence from our native orange–450 and acid blue–900 samples (See Appendix II for details about previously attempted photometric measurements). However, we have been able to determine rates of DPBF degradation in the presence of $^1O_2$ to characterize the $^1O_2$ quenching abilities of our βC and βC-AC, but with inconclusive results. In future studies, we hope to clarify and confirm the results found in our chemically based techniques with the implementation of a modified photometric technique, which we believe will provide much more clean and conclusive results. We believe this will be so because with our chemically based technique, the addition of another chemical to our solutions, DPBF, causes difficulties in solution preparation and possible chemical interactions with DPBF unrelated to $^1O_2$. However, our photometric technique will allow direct characterization of the quenching abilities of βC and βC-ACs by directly measuring the intensities of $^1O_2$ in solution at 1270nm.

During the course of this research, a secondary goal evolved—to generate new insights into the chemical nature of the blue–900 βC–TFA complexes and βC–TFA degradation products [6-8, 12] (See Appendix III for details). This secondary goal will be central to future experimental and theoretical studies (in the latter of which will attempt to fit the absorption spectra of βC–TCA complexes to various possible molecular structures using advanced electronic structure computations).

EXPERIMENTAL METHODS

A. Purification of Chemicals

βC (Sigma-Aldrich Type I, synthetic, ≥93%) was purified using standard column chromatographic protocols developed in Dr. Masthay's laboratory. [13] All other chemicals were used as purchased.

B. Chemical Optimization of Sensitizer + βC + Solvent and Sensitizer + βC + Acid + Solvent Combinations

As detailed below, optimal conditions for the solutions were determined for our experiments. Our solutions are made up of $5*10^{-5}$M C_{60} (the $^1O_2$ sensitizer) in benzene solvent with 10^{-5}M βC in either the absence or presence of 0.82M TCA (a >50,000-fold molar excess).[12] A pulsed Nd:YAG laser is used to irradiate these solutions to generate $^1O_2$. In our chemically based studies, DPBF at a concentration of $3.45*10^{-5}$M is added to the solutions.

1. Solvent Optimization

Initially, the majority of the solutions were prepared in CH_2Cl_2 (CHROMASOLV® Plus, for HPLC, ≥99.9%) solvent because βC and C_{60} are both soluble in CH_2Cl_2. Unfortunately, however, βC photodegrades in CH_2Cl_2 and other chloroalkane solvents via photoinduced electron–transfer reactions;[13-15] our βC−CH_2Cl_2 solutions accordingly rapidly lost color upon irradiation. Hence, benzene (Sigma-Aldrich, for HPLC ³99.9%) was our ultimate solvent choice for two reasons: (1) βC and C_{60} are both soluble in benzene; and (2) βC is photostable in benzene.

2. Acid Optimization

A variety of solutions of 10^{-5}M βC and 0.5-0.8M acid in solvent (CH_2Cl_2 or benzene) were prepared. Ultimately, it was decided that trichloroacetic acid would be used throughout our experiments because it is soluble in benzene, able to efficiently create the βC-acid blue complexes and cause a shift in absorbance to >900nm, and does not induce degradation of DPBF. (See Appendix IV for detailed explanations of the various acids we attempted to use).

3. $^1O_2$ Sensitizer Optimization [17-22]

Previous work done in Dr. Masthay's lab using an alternative $^1O_2$ sensitizer, methylene blue, and its inability to successfully work in the presence of acid suggested to us that a different $^1O_2$ sensitizer was necessary (See Appendix V for details of previous work conducted). This led us to the decision to try C_{60} (Sigma-Aldrich, 99.5%), which was ultimately used for a variety of reasons: (1) it's aromatic, nonpolar structure makes it unlikely to be protonated by acid; (2) it is relatively soluble in benzene; and (3) it is expected to generate a significant amount of $^1O_2$.

4. Concentration Optimization

In accord with the method of Mortensen and Skibsted [12] our optimized solutions are made up of 10^{-5}M βC and ~0.5M acid in benzene, similar to the concentrations used in their experiments: 10^{-5}M βC and 0.82M TCA in benzene (50,000-fold molar excess of TCA). These conditions were ideal because of the far-red shift in the βC–TCA complexes (λ_{max}~900nm) present with these concentrations. $5*10^{-5}$M C_{60} appears optimal for our experiments because we anticipate that its concentration is high enough to cause a reaction with DPBF (in chemical techniques) and to generate a detectable $^1O_2$ 1270nm signal (in photometric techniques). [17-22] $3.45*10^{-5}$M DPBF

was optimal for our chemically based experiments because it allows for obedience to Beer's Law with A_{416} <1.25.

C. Determination of $^1O_2$ quenching abilities of βC and βC-acid complexes using chemically-based techniques

Since it was determined that the *NIRQuest* proved to be insufficient at detecting the $^1O_2$ signals resulting from our solutions, we switched to an alternative, chemically-based technique. 1,3-diphenylisobenzofuran (DPBF) was chosen as our $^1O_2$ substrate; we used it as a means to measure the amount of $^1O_2$ present in solutions based on its degradation. DPBF proved to be sufficient as a $^1O_2$ substrate because it was soluble in our solvent (benzene), stable in our acid (TCA), and does not degrade in the absence of all sources of light.

DPBF has a natural absorption peak (λ_{max}) of 416nm. When DPBF is in the presence of $^1O_2$, the $^1O_2$ reacts with the furan ring of DPBF, forming a stable dicarbonyl product which does not absorb light in the visible range. The degradation of DPBF at 416nm, therefore, is used to determine the amount of $^1O_2$ present in solutions because the more $^1O_2$ is in solution, the more of these new dicarbonyl products will be formed, and DPBF will show a greater extent of degradation. This technique allows us to test our hypothesis since the degradation of DBPF is proportional to the amount of $^1O_2$ and inversely proportional to $\Phi_Q(^1O_2)$, quenching efficiency of βC and βC-TCA.

1. Effects of light on DPBF

2,6-Diphenylisobenzofuran (DPBF; Sigma-Aldrich, 97%) is commonly used as a $^1O_2$ substrate. We accordingly used DPBF to quantify $^1O_2$ in our solution. Even so, we found that quantification of $^1O_2$ with DPBF may yield results of limited reliability. When

yellow-blue solutions of DPBF in benzene were placed in quartz cuvettes, the solution turned colorless over time. For example, upon exposure to direct sunlight (mid-morning, July, Dayton, Ohio, 39.7589°N, 84.1916°W), the DPBF absorption peak was completely eliminated and the solution became colorless within 3 minutes.

Similar results were obtained with ambient (overhead fluorescent) light (although the loss of absorbance and color was slower with ambient light). Surprisingly, the rate of degradation was roughly the same in both aerated and sparged (*i.e.*, deoxygenated) solutions, indicating that $^1O_2$ does not play a role in this self-photodegradation process. The reaction appears to be a direct photodegradation reaction of DPBF, in which DPBF either (1) directly decomposes in an oxygen−and solvent−independent fashion; or (2) reacts with benzene. To confirm that this degradation is initiated by light, two cuvettes of DPBF in benzene were prepared; one was placed in a dark drawer and the other was placed in ambient light overnight. The next morning, the cuvette in the dark retained the same color as when it was originally prepared, whereas the cuvette that had been in the light had lost its coloration completely. Clearly then, DPBF is photolabile in benzene.

It was determined that the degradation of DPBF is completely light-dependent. Hence, all further experiments were conducted in the absense of all light (besides red lights in preparation of solutions).

D. Lab Methods and Techniques

Because of the light-induced degradation of DPBF, all solution preparation and experimental runs were conducted in the dark with red lights being our only source of light. Our solutions were prepared using the techniques described in Appendix VI. All experimental runs were done with solutions in a Starna Cells 6Q 1cm pathlength cuvette.

Our solutions were irradiated with 532nm pulses of the Nd:YAG laser at 15 second intervals at 10mJ/pulse. Throughout preparation of solutions and experimental runs, a stir bar was placed in the cuvette and the cuvette was placed on a stir plate to ensure thorough and continous mixing of the solutions. After each interval, an absorption spectrum was taken using only the Tungsten lamp (D_2 lamp is turned off), measuring the absorption of DPBF at 416nm. Figure 4 shows an experimental run measuring the degradation of DPBF at 416nm at 15 second time intervals of exposure to 532nm pulse laser. All runs were conducted at ambient room temperature (22°C).

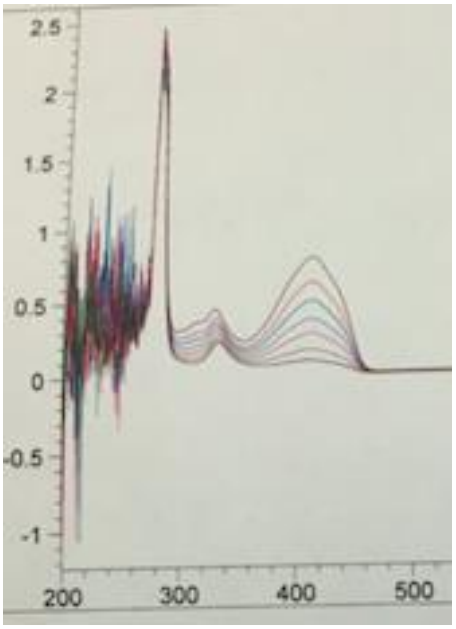

Figure 4. Absorption spectrum of DPBF+C_{60} in benzene solvent. Shows the degradation of DPBF at 416nm. These absorbances at 416nm (A_{416}) were then used in data analysis to determine degradation rates of DPBF. Spectra were taken at 15 second intervals of exposure to 532nm pulsed-laser.

Four different solutions were prepared in order to perform experimental runs: (1) DPBF+ C_{60}; (2) βC +DPBF+ C_{60}; (3) βC +TCA+DBPF+ C_{60}; and (4) TCA+DPBF+ C_{60}. Solutions of TCA, DPBF, and C_{60} were prepared and tested in order to verify that TCA didn't react with DPBF and cause any oxygen dependent degradation of DPBF, which could cause inconsistencies with our results. After solutions were prepared in a 6Q cuvette, an absorption spectrum was taken (time 0s). Then, the cuvette was placed in a

cuvette holder to be irradiated with the 532nm pulses of the laser. The laser was set at 10mJ/pulse, and hit a 90 degree beam splitter before hitting the cuvette, so the solution only received 10% of the total laser intensity. The solutions were irradiated for 15 second intervals, with an absorption spectrum taken after each interval. This was done until the solutions were irradiated for a total of 90 seconds (total of 7 absorbance measurements).

Data Analysis and Results

The absorbance of DPBF was monitored at 416nm at 15 second intervals of laser exposure. The natural log of these absorbances were taken and plotted versus total exposure time. These linear plots showed negative slopes, and confirmed first order kinetics. The slopes of these plots were used as DPBF degradation rates for the purpose of our experiment. R^2 values were also recorded to show how close the data are to the fitted regression line.

Subsequent to this data analysis, we normalized these data points to further confirm these results. The data was normalized for the concentrations of DPBF and C_{60} (by dividing the rate by the average A_{416} and A_{355} values, respectively, over an irradiation interval) for each run. These results are not shown here, but will be demonstrated in future papers.

Experimental runs were conducted over various days:

DPBF+ C_{60}

Date	Rate Constant (k)	R^2 Value
7/28/17	0.0142	0.99931
7/28/17	0.0139	0.99989
7/28/17	0.0134	0.99918
9/4/17	0.0136	0.99934
9/5/17	0.0234	0.99715
9/5/17	0.0277	0.97793
Average	0.0177	0.99547

βC+DPBF+ C_{60}

Date	Rate Constant (k)	R^2 Value
7/28/17	0.0054	0.99872
7/28/17	0.0049	0.99601
7/28/17	0.0065	0.99482
9/4/17	0.0079	0.99964
9/5/17	0.0080	0.99218
9/5/17	0.0071	0.99886
Average	0.0066	0.99671

βC +TCA+DBPF+ C_{60}

Date	Rate Constant (k)	R^2 Value
7/28/17	0.0100	0.99429
7/28/17	0.0074	0.99824
7/28/17	0.0069	0.99957
9/4/17	0.0076	0.99937
9/5/17	0.0066	0.99560
9/5/17	0.0061	0.99785
Average	0.0074	0.99749

TCA+DPBF+ C_{60}

Date	Rate Constant (k)	R^2 Value
8/1/17	0.0198	0.99926
8/2/17	0.0339	0.97245
8/2/17	0.0221	0.99488
8/2/17	0.0316	0.98264
9/4/17	0.0134	0.99283
9/5/17	0.0135	0.99412
9/5/17	0.0205	0.99256
9/5/17	0.0163	0.99759
Average	0.0168	0.99079

Average rate constants

Solution	Average rate constant
DPBF+ C_{60}	0.0177
βC +DPBF+ C_{60}	0.0066
βC +TCA+DBPF+ C_{60}	0.0074
TCA+DPBF+ C_{60}	0.0168

These average rates of DPBF degradation showed that solutions of DPBF+ C_{60} had the fastest rate of degradation, βC +DPBF+ C_{60} showed the slowest rate of degradation, and βC+TCA+DPBF+ C_{60} showed an intermediate rate of degradation. The TCA+DPBF+ C_{60} solutions showed a rate of degradation that was very similar and comparable to DBPF+ C_{60} alone solutions, indicating that TCA does not damage DPBF. Figure 5 shows the average rates plotted on a graph as the natural log of the absorbance over exposure time to laser.

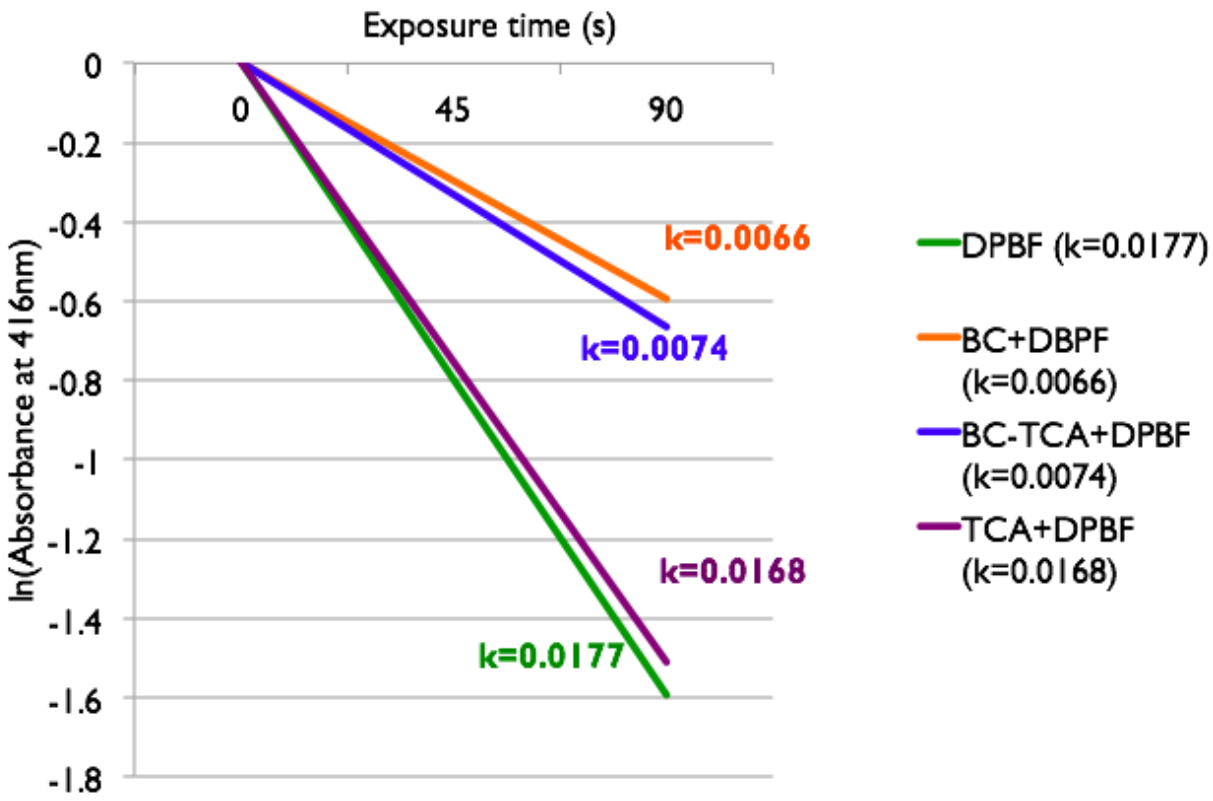

Figure 5. Based on the average rate constants (slopes), it is clear that DPBF alone (green line) has the fastest rate of degradation (compared to βC+DPBF+C_{60} and βC+TCA+DPBF+C_{60}), βC+DPBF+C_{60} (orange line) has the slowest rate, and βC+TCA+DPBF+C_{60} (blue line) has an intermediate rate constant. The TCA+DPBF+C_{60} (green line) solution showed a rate constant very similar to DPBF+C_{60}.

Discussion

Based on the average rates of degradation from each solution, our results matched our hypothesis. The DBPF and C_{60} alone solutions resulted the fastest rate of degradation, meaning that there was more $^1O_2$ present in these solutions compared to the other solutions. This result follows because a $^1O_2$ quencher was absent in these solutions, so a maximum amount of $^1O_2$ reacted with the DPBF, causing its degradation. The solutions with βC, DPBF, and C_{60} resulted in the slowest rate of degradation. This result follows because βC is effectively quenching $^1O_2$ in these solutions, so there is less $^1O_2$ left in solution to cause the degradation of DPBF. The solutions with βC, TCA, DPBF, and C_{60} showed an intermediate rate of degradation, which supported our hypothesis that βC-acid complexes would be less efficient at quenching $^1O_2$ than native βC. This occurred because we believe that the addition of acid to βC solutions induce a change in the electronic structre of to βC (modification of the energy of its triplet sate T_1) that causes it to be less efficient at deactivating $^1O_2$. Although the βC-acid complex solution did show a slightly faster rate of degradation, it wasn't to the extent that we anticipated. It was clearly seen by looking at the rates of degradation that the βC-acid complex was also unexpectedly relatively efficient at quenching $^1O_2$. There was not a large enough difference in the rates to prove to be completely significant and conclusive, so further tests are planned to be done to validate these results. (This result suggests that the energy of the T_1 state is insensitive to the protonation state of βC).

As noted above, solutions of TCA, DPBF, and C_{60} were prepared to determine if TCA caused acid-induced degradation to DPBF. Although these rates were not completely identical, we concluded that they were similar enough to prove that DPBF is

stable in the presence of TCA. We were further convinced this was the case because of the excess amount of TCA in the solutions (>50,000-fold molar excess). If the TCA was inducing degradation of DPBF, we would then have seen the same rate of degradation for our βC +TCA+DPBF+ C_{60} solutions, since these solutions have an equally great excess of acid present in solution. Therefore, we concluded that the TCA posed no problems to our experiments, allowing us to reach with confidence the unexpected conclusion that $\Phi_Q^{\beta C} \sim \Phi_Q^{\beta C + TCA}$.

Future Studies

In order to obtain more conclusive and significant results, photometric techniques will be used to characterize the efficiencies of βC and βC -acid complexes at deactivating $^1O_2$. This will be done used a cooled photomultiplier tube to directly measure the resulting $^1O_2$ phosphorescence signal at 1270nm. This technique will remove DPBF from our experiments, resulting in a cleaner, more accurate way to test our hypothesis to get more conclusive results.

A secondary experiment to be performed in the future would be to continue research attempting to study and determine the structure of the βC-acid complexes created in the lab. Experimental and theoretical studies will be conducted to characterize the molecular structures of these complexes using electronic structure computation. This research would be done to gain more insight into the structure of the pink-515nm BC that occurs during photosynthesis and the effect this has on the ability of βC to quench $^1O_2$.

Appendix I: βC in Photosystem II

βC plays the photoprotective role in green plants of quenching, or deactivating, $^1O_2$ that is produced as a byproduct in photosynthesis. βC is located in Photosystem II (PSII), which is located in the thylakoid membrane of plants and is the first protein complex that takes part in photosynthesis. Within PSII there is another species, chlorophyll, which is a green pigment responsible for the absorption of light to start the process of photosynthesis.

What is believed is occurring during photosynthesis in PSII is that the absorption of sunlight by chlorophyll causes the excitation of electrons within the photosystem. These excited electrons then cause water that is present in PSII to be "split", resulting in free protons and triplet oxygen. This triplet oxygen is oxygen's natural, stable state.

When chlorophyll is absorbing light from the sun, this causes the chlorophyll molecules to be excited from its stable, singlet state into its more excited triplet state. This triplet state chlorophyll, when in the presence of of triplet oxygen, through intersystem crosses, causes the production of $^1O_2$. Oxygen's singlet state is extremely toxic to the plant and can cause extreme oxidative damage.

As $^1O_2$ is generated, it is diffusing throughout PSII and passes by βC that is embedded in the membrane. βC reacts with the $^1O_2$ diffusing throughout the photosystem, and is able to convert it back to its more stable, triplet state before it can cause oxidative damage to the plants.

βC is very efficient at its role of quenching $^1O_2$ as it is produced in PSII. However, a specific phenomenon that occurs to βC during photosynthesis, The 515nm Effect, has been shown to possibly decrease βC's ability to quench this $^1O_2$.

The free protons that are generated from the splitting of water during photosynthesis must be pumped out of PSII to generate ATP. When these protons are being pumped out of PSII, they pass by the βC molecules that are embedded in the membrane. When the protons are passing by βC, this causes a structural change in βC, causes βC's absorption spectrum to change and shift its λ_{max} from 450nm to 515nm (The 515nm Effect). Our research focuses on the 515nm Effect and the effect that this structural change has on βC's ability to quench $^1O_2$.

Appendix II: Previous Attempts to Observe 1270nm $^1O_2$ Phosphorescence

$^1O_2$ Phosphorescence Signal and Characterization

We attempted to characterize $\Phi_Q^{orange\text{-}450}$ and $\Phi_Q^{blue\text{–}900}$ using a state–of–the–art transient near infrared emission spectrophotometer (Ocean Optics *NIRQuest*). More specifically, the $^1O_2$ generator buckminsterfullerene (C_{60}; Sigma-Aldrich, 99.5%) was added to solutions of βC and serially diluted to concentrations of $5*10^{-5}$M C_{60}. $^1O_2$ was generated by irradiating these βC + C_{60} and βC–TFA + C_{60} solutions with the 532nm pulsed Nd:YAG laser. We then attempted to monitor the intensity I_{1270} of the resulting 1,270nm emission of $^1O_2$[23] emanating from these solutions using an Ocean Optics *NIRQuest* Spectrophotometer operating in Edge Trigger mode (with 532nm laser pulses). Since I_{1270} is proportional to the concentration of $^1O_2$ in solution, this intensity was expected to be inversely proportional with the $^1O_2$–quenching efficiencies: $I_{1270} \propto \Phi_Q^{-1}$.

NIRQuest Operation

An Ocean Optics *NIRQuest* Spectrophotometer (a germanium photodiode array-based transient infrared spectrometer with an operating range of 900-1700nm) was selected for our experiments for three reasons. First, its operating range encompasses the anticipated 1270nm $^1O_2$ emission signal. Second, the *NIRQuest* interfaces easily with our pulsed Nd:YAG laser. Third, its cost ($16,000) was fundable using Chemistry Department funds.

The *NIRQuest* was triggered by the 20ns rising edge of a trigger pulse from the sync/out on the laser power supply, which is generated at the same time as the 6.5ns, 532nm pulses. The laser operates at a frequency of 10Hz; hence pulses come at 0.1 sec (10^5 μs) intervals. $^1O_2$ has an optical lifetime of 10^{-5}s (10μs), so that each 1270nm

phosphorescence signal comes ~10μs after the trigger, but is complete long before the next laser pulse reaches the sample. The *NIRQuest* thus integrates the 1270nm signal on a pulse-by-pulse basis.

Unfortunately, a solution of C_{60} (Sigma-Aldrich, 99.5%) in benzene produced no $^1O_2$ signal (see Fig. 4) because C_{60} does not absorb the 532nm second harmonic pulse ($\varepsilon_{532}(C_{60})$~0; see Fig. 5) from our pulsed Nd:YAG laser (Spectra Physics INDI-40-10). Because we wanted to confirm the existence of a 1270nm $^1O_2$ phosphorescence signal before changing the dichroic optics of the laser to the 355nm option, a temporary alternative $^1O_2$ sensitizer (Rose Bengal, which does absorb the 532nm pulses) in ethanol solvent was used.

Rose Bengal

A solution of Rose Bengal (Allied Chemical) in ethanol (AAPER Alcohol, 95%) produced a broad, asymmetric emission signal extending from 1100−1300nm with a peak at 1170nm and a shoulder at 1270nm (see Fig. 7). Though this signal encompasses the range of wavelengths expected for $^1O_2$, the signal does not originate from $^1O_2$—for two reasons: (1) the 1170nm signal does not match the emission spectrum of $^1O_2$ [17-22]; and (2) the intensity of the 1170nm signal was identical in air−saturated solutions ($[O_2]=1.91\times10^{-3}$M at 25°C), O_2−saturated solutions generated by bubbling with O_2(g) for 30 minutes prior to irradiation ($[O_2]=9.12\times10^{-3}$M) [24], and solutions sparged with high purity (99.998%) Ar(g) [24] prior to irradiation ($[O_2]$~0M). Thus, the 1170nm signal was independent of oxygen concentrations.

Furthermore, the signal does not originate from Rose Bengal, the solvent, or impurities in either. Nor does it originate from thermal lensing of blackbody emission, for the reasons detailed below.

First, the signal clearly originates in some way from Rose Bengal, since (i) low Rose Bengal concentrations resulted in no I_{1270} signals, and (ii) very high Rose Bengal concentrations also produced no signals (because the laser pulse was absorbed entirely at the entry edge of the cuvette, and hence did not pass by the fiber optics portal at the middle of the cuvette).[25]

Second, the signal does not originate from fluorescent or phosphorescent impurities in the solvent, since the signal was observed only in the presence of Rose Bengal; the signal was absent for neat ethanol. Even so, the signal was not due to emission from Rose Bengal [20] or Rose Bengal photoproducts (which manifest no emission from 1050-1100nm [*i.e.* near the short-wavelength edge of the 1170nm signal]) upon excitation with 532nm using a Varian Cary 1 Eclipse Fluorimeter (which has an upper wavelength range of 1100nm).[26]

Third, the signal cannot originate from a thermal lens generated via thermal relaxation of Rose Bengal following photoexcitation, for two reasons: (1) though a thermal lens could cause the beam to expand and intersect with the entry portal of the fiber optic cable with each pulse, resulting in a transient signal, the signal would occur at the actinic wavelength (532nm), which lies outside the spectral range of the *NIRQuest*, and hence would not be observed; and (2) the maximum temperature rise which would be generated by our 14mJ laser pulses in the irradiated beam volume of would be ;

(calculated assuming $mole^{-1}$ K^{-1} and = .789 g mL^{-1}).[20] This small temperature rise would seem to make a thermal lens unlikely.

Fourth, the signal appears to be independent of laser intensity.

Fifth, the 1170nm signal cannot originate from blackbody emission from the Rose Bengal [20] or ethanol, since at ambient temperature (21°C in our laboratory) the blackbody emission maximum is 9,860nm, according to the Wien displacement law . The observed emission maximum of 1170nm corresponds to a temperature of ~2,500K, which is clearly unattainable in our samples (0.0114 K temperature rise, as detailed above)—even if all of the absorbed laser energy were deposited into the sample as heat [20]. Hence, at this point, the nature of the 1170nm signal remains ambiguous. We accordingly plan to begin studies using C_{60} in benzene with a focused 355nm Nd:YAG third harmonic beam to see if we obtain 1270nm $^1O_2$ phosphorescence signals. [17-22]

Appendix III: Chemical Characterization of βC–TFA Complexes and βC–TFA Degradation Products

The structures of βC–ACs [6-8] in general and of βC–TFA complexes and βC–TFA degradation products in particular [12] are poorly characterized. Accordingly, a secondary goal of our experiments was to characterize the chemical properties of the βC–TFA complexes and βC–TFA degradation products [12] using a combination of vacuum and thin layer chromatographic (TLC) methods.

βC–TFA complexes

A solution of βC–TFA in benzene was prepared and then immediately dried under vacuum (~2-3 torr). When all the solvent had evaporated, an orange oil remained in the bottom of our 25mL round bottom flask. This product was dissolved in benzene, and an absorption spectrum was obtained. The spectrum showed a peak similar—but not identical—to that of pure βC; the wavelength maxima of the vibronic peaks were shifted to slightly longer wavelengths and their relative intensities were altered, suggesting that the orange vacuum product was similar, but not identical, to βC (see Fig. 6).

βC–TFA degradation products

Another solution of βC–TFA in benzene was prepared and incubated for 24 hours in the dark. As βC–TFA complexes are known to degrade over time [12] an absorption spectrum was taken to insure the 900nm peak of the βC–TFA complexes had disappeared. To characterize the colorless polar products, fluorescent silica gel TLC plates were then run with benzene as the mobile phase. Residual βC was the mobile and moved with the solvent front, (this compound showed an absorption identical to that of

βC when it was extracted from the TLC plate), whereas the βC–TFA degradation product was the immobile (R_F=0).

To further characterize the polar degradation products, preparative TLC was used. The immobile spot on the plate was scraped off and the immobile (in benzene) products were dissolved in 90% ethyl acetate/10% methanol. A second TLC plate was run of this immobile substance, but with 90% ethyl acetate/10% methanol as the mobile phase. The βC–TFA degradation products were mobile (displaying one spot that moved with the solvent front), thus confirming that the βC–TFA degradation products are polar, unlike βC.

Appendix IV: Acid Optimization

Sulfuric acid

Sulfuric acid (H_2SO_4; Fischer Scientific, Certified ACS Plus) was problematic because two layers formed upon adding H_2SO_4 to the 10^{-5}M βC solution in CH_2Cl_2. The formation of the two layers was not ideal for our experiments—even though both layers were blue—because it was difficult to determine the composition of each layer. Since the density of H_2SO_4 (1.84 g/cm^3) is greater than that of CH_2Cl_2 (1.33 g/cm^3), the bottom layer of the solution was presumably composed of H_2SO_4 and βC; however, it was uncertain if CH_2Cl_2 was also present in this bottom layer. The top layer was presumably comprised of CH_2Cl_2 and blue βC–H_2SO_4 complexes. Ultimately, because (1) βC is photolabile in CH_2Cl_2; and (2) we believe CH_2Cl_2 is present in both H_2SO_4 layers, it was decided that H_2SO_4 would not be the ideal acid for our experiments.

Nitric and Methanesulfonic Acid

Similar results were obtained when nitric (HNO_3; Fischer Scientific, Certified ACS Plus) and methanesulfonic (CH_3SO_3H, Sigma-Aldrich, 99%) acids were added to 10^{-5}M βC solutions in CH_2Cl_2. In the case of HNO_3, the solution initially became blue, but over a short period of time formed a yellowish/brown top layer and a colorless bottom layer, consistent with reports in the literature.[16] Presumably, the bottom layer was primarily composed of HNO_3, since the density of HNO_3 is 1.5129 g/cm^3 (greater than that of CH_2Cl_2). Apparently, βC was absent from the bottom layer (since it showed no coloration), which is possibly due to the moderate polarity of HNO_3, which has a dipole moment of 2.17±0.02D. The βC−CH_3SO_3H solution was similar to the βC−H_2SO_4 solution in that it formed two blue layers.

Trifluoroacetic acid (TFA)

TFA (also CF_3COOH; Sigma-Aldrich, 99+% Spectrophotometric grade) became our acid of choice during our initial photometric techniques using the *NIRQuest* photometer because it formed one, blue (λ_{max}~900nm) uniform layer when mixed with the βC in both benzene and CH_2Cl_2. However, when we switched to our chemically based techniques using DBPF, TFA ended up being problematic. TFA was shown to cause oxygen independent degradation of DPBF in solution by a chemical reaction between the DPBF and acid. Based on this finding, TFA proved to be insufficient as our acid of choice for our DPBF runs; however, TFA may be used again in the future with our new photometric experiments.

Gas Acids: Hydrochloric, Hydrobromic, and Hydroiodic acid

Based on experiments previously done in Dr. Masthay's lab with BC-acid complexes, the monoprotic acid HCl was tested in our βC solutions. (HBr and HI were also tested). With the help of Dr. Jeremy Erb, a bubbling apparatus was assembled in Dr. Masthay's lab to create these acid gases to bubble into our solutions. It was decided to use the gas form of these acids, opposed to the liquid form, because these acids are relatively insoluble in benzene. Bubbling the solutions with acid gas, however, would ensure optimal mixing and solubility of the acid in our benzene solvent. Also, it was decided to use these acids because we assumed that the monoprotic acids would dissociate almost completely in solution, eliminating excess HCl, HBr, or HI in solutions and resulting in many free protons and anions.

Bubbling Apparatus

An apparatus was set up with the help of Dr. Erb in order to bubble gas of various acids (HCl, HBr, and HI) into our cuvette. ~5-10g of our various salts (NaCl, KBr, and KI) were weighed and placed in our RBF. A stir bar was placed in the RBF in order to stir and speed up the reaction taking place in the RBF. ~5-10mL of sulfuric acid was poured into the burette above the RBF sealed tight. Our RBF contained two necks: one that connected to the burette and another that lead to rubber tubing and a needle that allowed the gas produced to enter the cuvette. Another needle was placed in the cuvette that was connected to more tubing, which lead to a beak filled with DI water and sodium carbonate, to neutralize excess gas produced.

The reaction between the salt and sulfuric acid produced the desired acid as a gas.

Hydrochloric Acid

5g of NaCl was placed in the RFB. A cuvette with a βC in benzene solution was hooked up to the bubbling apparatus and sulfuric acid was slowly dropped into the NaCl. The βC solution started out its normal orange color, and after bubbling for ~10-15 minutes, it turned a fainter orange (but still about the same color). Also, the solution appeared to turn turbid. The spectrum of the solution shows a slight peak at 880nm, which rises at first, then begins to fall over time. Also, the βC peak seemed to change shape, shift to shorter wavelengths, and decrease in absorbance over time. This could suggest that the H+ and Cl- ions are adding across the double bonds of the βC. The physical observation of the solution, along with the spectrum taken, suggested that this would not be ideal circumstances for our experiments.

It was suggested our problem could be caused by our solvent, benzene, so further tests were performed using dichloromethane (CH_2Cl_2). Since the temporary change was

made to using CH_2Cl_2 as our solvent, which was shown to cause degradation of BC upon radiation of the 532nm pulses of the Nd:YAG laser, the remaining tests using gas acids in CH_2Cl_2 solvent were to be performed using the 334nm lines of the Hg lamp.

When solutions of DPBF and C_{60} were prepared and bubbled with HCl gas, this caused a change in the structure of DPBF. This proved to be problematic towards being able to measure the degradation of DPBF for our studies, so HCl was ruled out as a potential acid for our experiments.

Hydroiodic Acid

The same bubbling apparatus was assembled and used for the production of HI gas from sodium iodine and sulfuric acid. Solutions of βC in both benzene and CH_2Cl_2 were prepared and bubbled with HI gas. It was determined that with both of these solutions, after bubbling for 10-15 minutes, the βC peak slightly decreased at 450nm, but at an extremely slow pace. It appeared that bubbling with HI was not solvent dependent, as it was with HCl; however, this could have been due to the fact that the βC-HI interaction was an extremely slow process or the iodide is unable to produce the βC-acid complex in the way our experiment requires. Due to these results, it was decided that HI would not be used to create our βC-acid blue complexes because it is either unable to or it is an extremely slow process.

Hydrobromic Acid

Next, using the same bubbling techniques described above for HCl, using sodium bromide and sulfuric acid to create HBr gas. The spectrum showed significant changes in the absorption spectrum of βC, making it unable to serve as our acid.

Trichloroacetic Acid

Since our bubbling techniques to produce gas acids proved to be insufficient in producing our βC-acid complexes, it was decided to find an alternative Bronsted acid for our experiments. Trichloroacetic acid (TCA) was chosen, since it is similar in composition to TFA, but does not cause oxygen-independent degradation of DBPF. A concentration of 0.82M was optimal for causing the complete shift in the absorption spectrum from 450nm to >900nm.

Appendix V: Prior Work with βC-acid Complexes

One of the main objectives of this research is to gain insights into the phenomenon of the 515nm Effect and its impact on βC's role in plants during photosynthesis. Previous research has been conducted in Dr. Masthay's lab studying this phenomenon using similar techniques currently used. Fritz Schomburg and Ryan Provost were my predecessors in Dr. Masthay's lab who, with the guidance and help of Dr. Masthay, originally came up with our chemical model of the 515nm Effect. They discovered that with the addition of acid to a solution of βC, the solution changed in color from its native color orange to a deep blue color. With the color change, they noticed a significant change in the absorption spectrum of the solution as well. The native orange solution of βC showed the characteristic absorption peak at 450nm; however, when acid was added to solution and caused the color change, the βC 450nm peak disappeared and bathochromically shifted in absorbance to 9890nm. It was thought that this shift in absorbance was caused by a change in the structure of βC with the addition of acid to solutions. It is still unclear exactly what this structure change entails, but future research in our lab is aimed at characterizing this.

In Dr. Masthay's lab, Schomburg and Provost were attempting to determine the effects the addition of acid had on βC's ability to quench $^1O_2$ in solution. In order to chemically determine this, methylene blue (λ_{max}=659) was used as a $^1O_2$ sensitizer. $^1O_2$ was generated in solution when the methylene blue was excited with the 632.8nm line from a 5mW He-Ne laser. 1,3-diphenylisobenzofuran (DPBF) was added to solutions and served as the $^1O_2$ substrate. DPBF, when in the presence of $^1O_2$, reacts with the $^1O_2$ by opening up the furan ring of DPBF and forming a stable dicarbonyl. The degradation of

DPBF on its absorption spectrum at 416nm was measured and used as a means to determine the amount of $^1O_2$ in each solution.

Through their experiment, they discovered that methylene blue proved to be unstable in the presence of DPBF. They were able to show that βC effectively quenches $^1O_2$, however, when acid was added to solutions with methylene blue, the protonated methylene blue in some unknown mechanism was unstable in the presence of the $^1O_2$ substate. Therefore, they were unable to characterize the $^1O_2$-quenching efficiency of the βC-acid complexes. The results and suggestions from their research greatly influenced the work of my experiments. From their conclusions, for my research I chose a nonpolar $^1O_2$ sensitizer (C_{60}) that was unable to be protonated, eliminating the problem Schomburg and Provost ran into. I also used their methods using DPBF to measure the amount of $^1O_2$ generated when conducting our chemically-based techniques. The results and difficulties this research presented directly led into my continuation and improvements of this research project.

Appendix VI: Solution Preparation

C_{60} Stock Solutions: $5*10^{-5}$M

0.0018g of C_{60} was weighed and added to 50mL of benzene. The solution was stirred with a stir bar on a stir plate to ensure thorough mixing. While the solution was mixed, it was placed on a hot plate set at 50°C until all of the solid C_{60} had dissolved in the benzene. This solution was used as the base of all our solutions. The concentration of this solution is $5*10^{-5}$M

DPBF Stock Solution: $3.45*10^{-5}$M.

0.0014g of DPBF was weighed and added to 25mL of benzene. This concentration is $2*10^{-5}$M. 0.5mL of this stock solution is added to 2.5mL of solution in the cuvette, making the concentration of DPBF in the cuvette $3.45*10^{-5}$M.

βC Stock Solution: 10^{-5}M.

0.0500g βC was weighed and dissolved in 10mL of benzene. A final concentration of 10^{-5}M was achieved by various serial dilutions.

DPBF+ C_{60} Solution

2.5mL of the C_{60} stock solution and 0.5mL of the DPBF stock solution is added to a 6Q 1cm cuvette.

DPBF+ C_{60} +βC Solution

0.1mL of the BC stock solution, 0.5mL of the DPBF stock solution, and 2.4mL of the C_{60} stock solution are added to a cuvette.

DPBF+ C_{60} +βC+TCA

0.1mL of the BC stock solution, 0.5mL of the DPBF stock solution, and 2.4mL of the C_{60} stock solution are added to a cuvette. 0.400g of TCA is weighed out in a beaker,

and the 3mL of solution in the cuvette is poured into the beaker containing TCA. This solution is mixed until no TCA crystals remain. Then, the solution is poured back into the same cuvette and a spectrum is immediately taken.

DPBF+ C_{60} +TCA

0.5mL of DPBF stock solution and 2.5mL of C_{60} are added to a cuvette.0.400g of TCA is weighed out in a beaker, and the 3mL of solution in the cuvette is poured into the beaker containing TCA. This solution is mixed until no TCA crystals remain.

Appendix VII: Hg Lamp Experiments

Hg Lamp 313nm Filter

Since C_{60} has a low extinction coefficient at 532nm, and it absorbs much greater at 313nm, it was decided to perform the same experiments with the Hg lamp to determine if this changed the results. It turned out that this did change our results, with the βC-TFA complex being the intermediate rate, and the βC being the slowest; however, the 313nm filter proved to be an ineffective way to test our experiments. It was determined that DPBF is very photolabile and degrades when it is exposed to wavelengths of light that it absorbs. DPBF has a relatively high absorbance at 313nm (~0.3), which poses problems to our experiments because some of the DPBF degradation is due to its photodegradation and not due to the degradation caused by the $^1O_2$ produced by C_{60}. Because of these results, it was decided that the laser would be the best choice for the excitation of the C_{60} to produce $^1O_2$ for our experiments.

Hg Lamp 436nm Filter

DPBF was shown to degrade when exposed to the 436nm filter of the Hg lamp. Its degradation was faster than with the 313nm filter, and this was suggested to be because DPBF has a higher absorbance at 436nm (0.80740). It was shown to degrade by a little more than half in 2 minutes. Next, a solution of DPBF in benzene was prepared and then bubbled with argon for 30 minutes. Its degradation was observed after exposure to the 436nm filter of the Hg lamp. This bubbled solution showed almost no degradation of DPBF (dropped in absorbance by ~0.04 in 5 minutes). From this result, it was concluded that the degradation of DPBF is dependent on the presence of oxygen. The

degradation of DPBF is therefore not caused by the generation of DPBF free radicals or self-degradation of DPBF in solution.

Acknowledgements

I would first and foremost like to thank Dr. Masthay for all of his help and support with my research over the past 2 years. I cannot thank him enough for all of the guidance he has given me while I have been his student in the classroom and conducting research in his lab. He has been an amazing thesis mentor in providing me with the necessary information to perform experiments and helping with the publication of this manuscript. I would also like to give a special thanks to Dr. Perry Yaney for all of his help with the *NIRQuest* in the Summer of 2016 and Dr. Erb for his assistance with creating our bubbling apparatus. I also thank the generous support of the Chemistry Department and University Honors Program for allowing me to be able to conduct my research over the years. A special thanks to the Berry Family and the Berry Family Foundation for financing my research and allowing me to stay on campus to conduct research during the Summer of 2016. And finally, an extra special thanks to my lab partners Ashlee Wertz, Jackson Huang, and Gifty Antwi for the countless hours we have spent together researching and performing experiments in the lab, all of which could not have been done alone. Thank you all for all of your guidance and support thoughout this process.

REFERENCES

1. Krinsky, N.I., Function, in *Carotenoids*, O. Isler, Editor. 1971, Birkhäuser: Basel. p. 669-716.
2. Duysens, L.N.M., Transfer of light energy within the pigment systems present in photosynthesizing cells. *Nature*, **1951**. 168: 548-550.
3. Telfer, A., What is b–carotene doing in the photosystem II reaction centre? *Phil. Trans. R. Soc. Lond. B* **2002**. 357: 1431-1440.
4. Govindjee, Carotenoids in Photosynthesis: An Historical Perspective, in *The Photochemistry of Carotenoids*, H.A. Frank, et al., Editors. 1999, Kluwer Academic Publishers: Dordrecht. p. 1-19.
5. Carr, F.H. and E.A. Price, Colour reactions attributed to vitamin A. *Biochem. J.*, **1926**. 20: 497-501.
6. Haugan, J.A. and S. Liaaen–Jensen, Blue carotenoids. Part I. Novel oxonium ions derived from fucoxanthin. *Acta Chem. Scand.*, **1994**. 48: 68-75.
7. Haughan, J.A. and S. Liaaen-Jensen, Blue carotenoids. Part 2: The chemistry of the classical colour reaction of common carotenoid 5,6 epoxides with acid. *Acta Chem. Scand.*, **1994**. 48: 152-159.
8. Britton, G., R.J. Weesie, D. Askin, J.D. Warburton, L. Gallardo-Guerrero, F.J. Jansen, H.J.M. DeGroot, J. Lugtenburg, J.P. Cornard and J.C. Merlin, Carotenoid blues: Structural studies on carotenoproteins. *Pure Appl. Chem.*, **1997**. 69: 2075-2084.
9. Wassermann, A., Proton–acceptor properties of carotene. *J. Chem. Soc.*, **1954**: 4329-4336.
10. Wassermann, A., Properties of ion–pairs formed by proton transfer to conjugated polyenes. *Trans. Far. Soc.*, **1957**. 53: 1029-1030.
11. Prum, R.O., A.M. LaFountain, C.J. Berg, M.J. Tauber and H.A. Frank, Mechanism of carotenoid coloration in the brightly colored plumages of broadbills (*Eurylaimidae*). *J. Comp. Physiol. B*, **2014**. 184: 651-672.
12. Mortensen, A. and L.H. Skibsted, Kinetics and mechanism of the primary steps of degradation of carotenoids by acid in homogeneous solution. *J. Agric. Food Chem.*, **2000**. 48(2): 279-286.
13. Wang, W., *Photochemical Characterization of the Intensity Dependence in Multiphoton-Reactive Systems: Application to the Photodegradation of b-Carotene*, 2008M.S. Thesis, Chemistry, University of Dayton, Dayton, OHpp.
14. Gurzadyan, G.G. and S. Steenken, Photoionization of b-carotene *via* electron transfer from excited states to chlorinated hydrocarbon solvents. A picosecond transient absorption study. *Phys. Chem. Chem. Phys.*, **2002**. 4(13): 2983-2988.
15. Fujii, R., Y. Koyama, A. Mortensen and L.H. Skibsted, Generation of radical cation of b-carotene in chloroform via the triplet state as revealed by time-resolved absorption spectroscopy. *Chem. Phys. Lett.*, **2000**. 326: 33-38.
16. Karrer, P. and E. Jucker, Carotenoids, E.A. Braude, Editor. 1950, Elsevier Publ. Co.: New York.
17. Hare, J.P., H.W. Kroto and R. Taylor, Preparation and UV/visible spectra of fullerenes C_{60} and C_{70}. *Chem. Phys. Lett.*, **1991**. 177(4,5): 394-398.

18. Snyder, J.W., E. Skovsen, J.D.C. Lambert, L. Poulsen and P.R. Peter R. Ogilby, Optical detection of $^1O_2$ from single cells. *Phys. Chem. Chem. Phys.*, **2006**. 8(37): 4280.
19. Andersen, L.K. and P.R. Ogilby, A nanosecond near-infrared step-scan Fourier transform absorption spectrometer: Monitoring $^1O_2$, organic molecule triplet states, and associated thermal effects upon pulsed-laser irradiation of a photosensitizer. *Rev. Sci. Instrum.*, **2002**. 73(12): 4313-4325.
20. Nagano, T., K. Arakane, A. Ryu, T. Masunaga, K. Shinmoto, S. Mashiko and M. Hirobe, Comparison of single oxygen production efficience of C_{60} with other photosensitizers, based on 1268 nm emission. *Chem. Pharm. Bull.*, **1994**. 42(11): 2291-2294.
21. Bilsky, P., B. Zhao and C.F. Chignell, $^1O_2$ phosphorescence photosensitized in nanoaggregates of C60 buckminsterfullerene is insensitive to solvent and quenchers and strongly red–shifted indicating highly polarizable interior. *Chem. Phys. Lett.*, **2008**. 458: 157-160.
22. Prat, F., C. Martí, S. Nonell, X. Zhang, C.S. Foote, R. González–Moreno, J.L. Bourdelande and J. Font, C_{60} fullerene–based materials as $^1O_2$ $O_2(^1D_g)$ photosensitizers: A time–resolved near–IR luminescence and optoacoustic study. *Phys. Chem. Chem. Phys.*, **2001**. 3: 1638-1643.
23. Krasnovsky, A.A.J., Y.V. Roumbal and A.A. Strizhakov, Rates of $^1O_2$ (^1D_g) production upon direct excitation of molecular oxygen by 1270 nm laser irradiation in air–saturated alcohols and micellar aqueous dispersions. *Chem. Phys. Lett.*, **2008**. 458: 195-199.
24. Murov, S.L., *Handbook of Photochemistry*. 1973, New York: Marcel-Dekker, Inc. 272.
25. Additionally, we noted that Rose Bengal degraded rapidly upon laser pulse intensities of 14mJ pulse^{-1}. However, with pulse intensities of 1.5mJ*pulse-1, the Rose Bengal degraded more slowly.
26. While it is possible that laser–induced two–photon excitation of Rose Bengal could result in NIR emission from Rose Bengal differing from the one–photon excitation emission induced in the fluorimeter, this possibility seems unlikely.
27. Zhang, X.F. and X. Li, The photostability and fluorescence properties of diphenylisobenzofuran. *J. Luminescence*, **2011**. 131: 2263-2266.